

## Evaluation of anti-podoplanin rat monoclonal antibody NZ-1 for targeting malignant gliomas<sup>☆</sup>

Yukinari Kato<sup>a,b,\*</sup>, Ganesan Vaidyanathan<sup>c</sup>, Mika Kato Kaneko<sup>a,b</sup>, Kazuhiko Mishima<sup>d</sup>, Nidhi Srivastava<sup>a</sup>, Vidyalakshmi Chandramohan<sup>a</sup>, Charles Pegram<sup>a</sup>, Stephen T. Keir<sup>e</sup>, Chien-Tsun Kuan<sup>a</sup>, Darell D. Bigner<sup>a</sup>, Michael R. Zalutsky<sup>c</sup>

<sup>a</sup>Department of Pathology, Duke University Medical Center, Durham, NC 27710, USA

<sup>b</sup>The Oncology Research Center, Advanced Molecular Epidemiology Research Institute, Yamagata University Faculty of Medicine, Yamagata 990-9585, Japan

<sup>c</sup>Department of Radiology, Duke University Medical Center, Durham, NC 27710, USA

<sup>d</sup>Saitama Medical University International Medical Center 1397-1 Yamane Hidaka-shi, Saitama 350-1298, Japan

<sup>e</sup>Department of Surgery, Duke University Medical Center, Durham, NC 27710, USA

Received 30 December 2009; received in revised form 4 March 2010; accepted 25 March 2010

### Abstract

**Introduction:** Podoplanin/aggrus is a mucin-like sialoglycoprotein that is highly expressed in malignant gliomas. Podoplanin has been reported to be a novel marker to enrich tumor-initiating cells, which are thought to resist conventional therapies and to be responsible for cancer relapse. The purpose of this study was to determine whether an anti-podoplanin antibody is suitable to target radionuclides to malignant gliomas.

**Methods:** The binding affinity of an anti-podoplanin antibody, NZ-1 (rat IgG<sub>2a</sub>), was determined by surface plasmon resonance and Scatchard analysis. NZ-1 was radioiodinated with <sup>125</sup>I using Iodogen [<sup>125</sup>I-NZ-1(Iodogen)] or *N*-succinimidyl 4-guanidinomethyl 3-<sup>131</sup>I iodobenzoate [<sup>131</sup>I]SGMIB-NZ-1), and paired-label internalization assays of NZ-1 were performed. The tissue distribution of <sup>125</sup>I-NZ-1 (Iodogen) and that of [<sup>131</sup>I]SGMIB-NZ-1 were then compared in athymic mice bearing glioblastoma xenografts.

**Results:** The dissociation constant (*K<sub>D</sub>*) of NZ-1 was determined to be  $1.2 \times 10^{-10}$  M by surface plasmon resonance and  $9.8 \times 10^{-10}$  M for D397MG glioblastoma cells by Scatchard analysis. Paired-label internalization assays in LN319 glioblastoma cells indicated that [<sup>131</sup>I]SGMIB-NZ-1 resulted in higher intracellular retention of radioactivity (26.3±0.8% of initially bound radioactivity at 8 h) compared to that from the <sup>125</sup>I-NZ-1(Iodogen) (10.0±0.1% of initially bound radioactivity at 8 h). Likewise, tumor uptake of [<sup>131</sup>I]SGMIB-NZ-1 (39.9±8.8 % ID/g at 24 h) in athymic mice bearing D2159MG xenografts in vivo was significantly higher than that of <sup>125</sup>I-NZ-1(Iodogen) (29.7±6.1 %ID/g at 24 h).

**Conclusions:** The overall results suggest that an anti-podoplanin antibody NZ-1 warrants further evaluation for antibody-based therapy against glioblastoma.

© 2010 Elsevier Inc. All rights reserved.

**Keywords:** Podoplanin; Monoclonal antibody; Malignant gliomas; SGMIB; Internalization; Biodistribution

### 1. Introduction

Gliomas are the most common primary brain tumors, and glioblastoma multiforme is the most frequent and malignant type of gliomas [1]. Despite advances in surgical techniques, radiation therapy and adjuvant chemotherapy, their prognoses remain poor. Many antigens, such as epidermal growth factor receptor (EGFRwt), its glioma-associated deletion variant EGFRvIII, lacto-series ganglio-

<sup>☆</sup> This study was supported by NIH grants CA42324, 5P50 CA108786, 5P50 NS20023 and R37 CA011898. Y.K. was supported by the Global COE Program for Medical Sciences, Japan Society for the Promotion of Science.

\* Corresponding author. Department of Pathology, Duke University Medical Center, Durham, NC 27710, USA. Tel.: +1 919 613 6154; fax: +1 919 684 6791.

E-mail address: [yukinari-k@bea.hi-ho.ne.jp](mailto:yukinari-k@bea.hi-ho.ne.jp) (Y. Kato).

sides, tenascin and chondroitin sulfate proteoglycans, have been found in gliomas, and up-regulation of those molecules has been observed in brain tumor cells [2–7]. Although these molecules are under investigation as therapeutic targets, multiple entities ultimately may have to be targeted for optimal therapy in order to compensate for tumor heterogeneity.

Podoplanin is a platelet aggregation-inducing factor [8–11] and its expression has been reported in many tumors including malignant brain tumors [12–23]. Importantly, recent investigations have suggested that expression of podoplanin is associated with tumor metastasis [24,25], malignant progression [15,22] and epithelial-mesenchymal transition [26]. Podoplanin expression has also been reported to be associated with clinical outcome [14,16–18,27,28]. In solid tumors such as brain tumors, only a small and phenotypically distinct subset of cells could be responsible for generating and sustaining tumors and thus be considered cancer stem cells or tumor-initiating cells (TICs) [29]. Because TICs are thought to be resistant to conventional therapies and are responsible for relapse, targeting TICs could be a promising approach to cancer therapy [30,31]. Podoplanin has been reported to be a TIC marker; therefore, immunotherapy using specific antibodies reactive to podoplanin may eradicate TICs in cancers [32].

We previously produced an anti-podoplanin antibody, NZ-1 [23,33]. NZ-1 should have not only high specificity and sensitivity but also high binding affinity against podoplanin to be applied for radioimmunotherapy or immunotoxin therapy. Furthermore, particularly for its use as an immunotoxin, NZ-1 should be internalized into tumor cells and also well accumulated into tumors *in vivo*. The object of this study was to determine the affinity of NZ-1 and to investigate whether NZ-1 is a suitable candidate for therapy against malignant gliomas by performing internalization assays *in vitro* using several glioblastoma cell lines and biodistribution experiments *in vivo* using glioblastoma xenograft models.

## 2. Materials and methods

### 2.1. General

All reagents were purchased from Sigma-Aldrich (St. Louis, MO, USA) except where noted. Sodium <sup>125</sup>I-iodide (2200 Ci/mmol) and sodium <sup>131</sup>I-iodide (1200 Ci/mmol) in 0.1N NaOH were supplied by Perkin-Elmer Life and Analytical Sciences (Boston, MA, USA).

### 2.2. Animals, cell lines and the xenograft model

Female athymic mice (nu/nu genotype, BALB/c background, 6 weeks or older) were used for all antitumor studies. Animals were maintained in Thoren filter-top cages (Thoren Caging Systems, Hazleton, PA, USA). All animal procedures conformed to Institutional Animal Care and Use

Committee and National Institutes of Health guidelines. The LN319 glioblastoma cell line was donated by Dr. Webster K. Cavenee (Ludwig Institute for Cancer Research, San Diego, CA, USA). D397MG and D245MG glioblastoma cell lines and the D2159MG xenograft were established at Duke University. D2159MG xenograft cells were dissociated with Liberase (Roche, Indianapolis, IN, USA) at a 100 µg/ml concentration. LN319 and D2159MG were cultured at 37°C in a humidified atmosphere of 5% CO<sub>2</sub> and 95% air in Dulbecco's Modified Eagle's Medium (Invitrogen Corp., Carlsbad, CA, USA), including 2 mM L-glutamine and 1% of a penicillin–streptomycin solution, and D397MG and D245MG were cultured in Zinc Option medium (Invitrogen) supplemented with 10% heat-inactivated fetal bovine serum (Sigma-Aldrich).

### 2.3. Anti-podoplanin monoclonal antibody NZ-1

The development of the anti-podoplanin mAb NZ-1 was described previously [23]. Briefly, Sprague-Dawley rats were immunized by neck subcutaneous injections of the synthetic peptide EGGVAMPGAEDDVV (hpp3851), corresponding to amino acids 38–51 of human podoplanin plus C-terminus cysteine conjugated with KLH with Complete Freund's Adjuvant (Difco Laboratories, Detroit, MI, USA). One week later, secondary intraperitoneal immunization was performed. The booster injection was given intraperitoneally 2 days before spleen cells were harvested. The spleen cells were fused with mouse myeloma P3U1 cells by using polyethylene glycol (Mr 4000); the hybridomas were grown in RPMI medium with hypoxanthine, aminopterin and thymidine selection medium supplement (Sigma-Aldrich). The culture supernatants were screened by ELISA for binding to the synthetic peptide. The characterization of NZ-1 was performed as in a previous study [23,33]. NZ-1 was produced in ascites of athymic mice and purified with a Protein-G column (Thermo Scientific, Inc., Rockford, IL, USA).

### 2.4. Flow cytometry

Glioblastomas cells were collected by trypsin-EDTA treatment and were incubated with NZ-1 (1 µg/ml) or isotype control (rat IgG<sub>2a</sub>) for 30 min at 4°C. Then the cells were incubated with an Oregon green-conjugated anti-rat antibody (1:200 diluted; Invitrogen) for 30 min. Flow cytometry was performed using a FACSCalibur instrument (Becton Dickinson, Franklin Lakes, NJ, USA).

### 2.5. Affinity determination by surface plasmon resonance

To determine the affinity, biotinylated podoplanin peptide (hpp3851) was immobilized on the surface of streptavidin chips for analysis by using the BIAcore 3000 system (BIAcore, Piscataway, NJ, USA). The running buffer was 10 mM HEPES, 150 mM NaCl and 3.4 mM EDTA (pH 7.4). The NZ-1 was passed over the biosensor chip, and affinity rate constants (association rate constant,  $k_{\text{assoc}}$ , and disasso-

ciation rate constant,  $k_{\text{diss}}$ ) were determined by nonlinear curve fitting using the Langmuir one-site binding model of the BIAevaluation software (BIAcore). The affinity constant ( $K_A$ ) at equilibrium was calculated as  $K_A = k_{\text{assoc}}/k_{\text{diss}}$ , and the dissociation constant ( $K_D$ ) was determined as  $1/K_A$ .

#### 2.6. Radiolabeling of NZ-1 with $^{125}\text{I}$ using Iodogen: $^{125}\text{I}$ -NZ-1(Iodogen)

A solution of NZ-1 (250–300  $\mu\text{g}$ ; 5 mg/ml) in phosphate buffer (pH 7.4) was added to a 2-dram vial coated with Iodogen (10  $\mu\text{g}$ ) followed by a solution of sodium [ $^{125}\text{I}$ ]iodide ( $\sim 1$  mCi; 2–3  $\mu\text{l}$ ). The mixture was incubated at room temperature for 10 min with occasional shaking, and the labeled protein was isolated by gel filtration on a PD-10 column (GE Healthcare, Piscataway, NJ, USA) using PBS as running buffer.

#### 2.7. Radiolabeling of NZ-1 with SGMIB

The radioiodinated prosthetic group was synthesized from the corresponding trialkylstannyl precursor and purified as previously reported [34]. For labeling with [ $^{125}\text{I}$ ]SGMIB or [ $^{131}\text{I}$ ]SGMIB, NZ-1 in borate buffer (pH 8.5; 50  $\mu\text{l}$  of 5 mg/ml) was incubated with 0.4–1.6 mCi (0.33–1.33 nmol) of the tracer at room temperature for 15–20 min, and the labeled NZ-1 ([ $^{125}\text{I}$ ]SGMIB-NZ-1 or [ $^{131}\text{I}$ ]SGMIB-NZ-1) was purified by gel filtration. The integrity of labeled NZ-1 was determined by gel filtration HPLC using a TSK2000SW column.

#### 2.8. Determination of immunoreactive fraction

The immunoreactivity of radiolabeled NZ-1 was evaluated by a magnetic bead assay [35] using streptavidin-coated MPG magnetic beads (Controlled Pore Glass, Lincoln Park, NJ, USA) coated with the biotin-labeled podoplanin peptide (hpp3851) or, to control for nonspecific binding, biotin-labeled BSA. Each labeled NZ-1 solution (5 ng in 50  $\mu\text{l}$  PBS) in triplicate was added to increasing volumes (25, 50 and 100  $\mu\text{l}$ ) of both positive and control beads in 115 mM phosphate buffer (pH 7.4) with 0.05% BSA and 0.05% Brij 35, and the percent of total radioactivity that bound to the beads was determined. The immunoreactive fractions were calculated by the method of Lindmo et al. [36].

#### 2.9. Scatchard analysis

A modified Scatchard analysis was performed to measure the binding affinity of  $^{125}\text{I}$ -NZ-1(Iodogen) against LN319 and D397MG glioblastoma cells. Cells were plated in 24-well plates at a density of  $5 \times 10^4$  per well and incubated overnight at 37°C in a 5%  $\text{CO}_2$  humidified atmosphere.  $^{125}\text{I}$ -NZ-1(Iodogen) was serially diluted from 8  $\mu\text{g}/\text{ml}$  and was incubated with podoplanin-positive glioblastoma cell lines LN319 and D397MG at 4°C for 4 h. The podoplanin-negative cell line D245MG was used as a negative control. The cell-bound radioactivity was measured as a proportion

of input activity, and nonlinear regression analysis was performed to calculate the dissociation constant ( $K_D$ ) with GraphPad Prism software (GraphPad Prism Software, San Diego, CA, USA).

#### 2.10. Internalization assay

The podoplanin-expressing cell lines or xenograft-derived cells used in these studies were LN319, D397MG and D2159MG. Cells were plated in six-well plates at a density of  $5 \times 10^5$  per well and incubated overnight at 37°C in a 5%  $\text{CO}_2$  humidified atmosphere. On the day of the assay, the cells were incubated at 4°C for 30 min. The assays were performed in a single- or dual-label format. Both labeled ( $^{125}\text{I}$  and  $^{131}\text{I}$ ; about 1  $\mu\text{g}$  each) NZ-1 mAbs were added to the wells, creating conditions of mAb excess. The cells were incubated at 4°C for 1 h, washed with fresh medium to remove unbound radioactivity and brought to 37°C. Cells were then processed at 0, 1, 2, 4, 8, 16 and 24 h as follows: acidic medium (zinc option, pH 2.0; 1 ml) was added to each well, and the cells were incubated for 10 min at 4°C. The acid wash was transferred to a counting vial, and the cells were further washed with 1 ml of the acidic medium and pooled with the previous wash. The cells were solubilized by incubation at room temperature with 0.5 ml of 0.5N NaOH overnight. Cell culture supernatant aliquots, acid washes and solubilized cell fractions were then counted in the gamma counter using a dual-label program.

#### 2.11. Biodistribution

Subcutaneous tumor transplantation was done in the right flank of the animals with an inoculation volume of 50  $\mu\text{l}$  using tumor homogenate from xenografts as previously described [37]. Groups of five mice were used for each time point of the studies. In the first experiment, performed in a paired-label format, mice were injected with 4.0  $\mu\text{Ci}$  each of  $^{125}\text{I}$ -NZ-1(Iodogen) and [ $^{131}\text{I}$ ]SGMIB-NZ-1 via the tail vein, and biodistribution of the radiolabeled mAb was determined at 6, 24, 48, 72, 144 and 192 h. A second experiment was conducted to determine the specificity of uptake. For this experiment, the control mice were injected with 4  $\mu\text{Ci}$  of [ $^{125}\text{I}$ ]SGMIB-NZ-1 with or without co-injection of a 100-fold excess of unlabeled NZ-1, and biodistribution was examined at 6, 24 and 48 h. At each time point, mice were killed with an overdose of isofluorane, and tumor and other organs of interest were harvested, blot-dried, weighed and counted in an automated gamma counter for  $^{125}\text{I}$  and  $^{131}\text{I}$  activity along with injection standards. The results are expressed as percent injected dose per gram of tissue (%ID/g). The statistical significance of the difference in uptake between the two tracers was calculated by a paired or unpaired Student's *t* test using the Microsoft Excel program statistical function. The differences were considered to be significant if the *P* values were less than .05.

### 3. Results

#### 3.1. Radiolabeling

NZ-1 was radiolabeled using Iodogen in almost quantitative radiochemical yields and with a specific activity of 3.9 mCi/mg. When SGMIB was used for radiolabeling, the conjugation yield was  $66.6 \pm 14.1\%$  ( $n=2$ ) with a specific activity of  $2.6 \pm 0.4$  mCi/mg. Size-exclusion HPLC indicated that more than 95% of the radioactivity was associated with a peak corresponding to the retention time of the intact mAb with little or no aggregation. Immunoreactive fractions for each batch of the labeled NZ-1 are given in appropriate subsections below.

#### 3.2. Kinetics of NZ-1 binding to podoplanin

To determine the affinity of NZ-1, we performed a kinetic analysis of the interaction of NZ-1 with a podoplanin peptide (hpp3851) by surface plasmon resonance (BIAcore). Determination of the association and dissociation rates from the sensorgrams revealed a  $k_{\text{assoc}}$  of  $3.2 \times 10^5$  (mol/L s) $^{-1}$  and a  $k_{\text{diss}}$  of  $4.3 \times 10^5$  s $^{-1}$ . The  $K_A$  at binding equilibrium, calculate as  $K_A = k_{\text{assoc}}/k_{\text{diss}}$ , was  $7.4 \times 10^9$  (mol/L) $^{-1}$ ,  $K_D = 1/K_A = 1.2 \times 10^{-10}$  (mol/L), indicating that NZ-1 has high-affinity binding to a podoplanin peptide. NZ-1 was also analyzed by conventional Scatchard analysis using podoplanin-positive glioblastoma cell lines LN319 and D397MG and a podoplanin-negative glioblastoma cell line, D245MG. Podoplanin expression in the positive cell lines was confirmed by flow cytometry (Fig. 1). For Scatchard

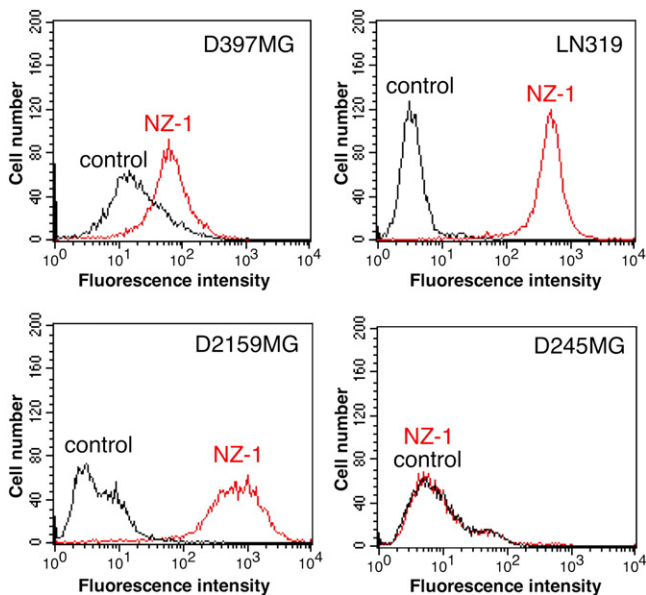


Fig. 1. NZ-1 recognition of podoplanin on the cell surface of glioblastoma cells by flow cytometry. D397MG, LN319, D2159MG and D245MG glioblastoma cells were collected by trypsin-EDTA treatment, and cells were incubated with NZ-1 or an isotype-matched control antibody (rat IgG<sub>2a</sub>). The cells were next incubated with an Oregon green-conjugated anti-rat antibody. Flow cytometry was performed using a FACSCalibur instrument.

analysis, NZ-1 was labeled with  $^{125}\text{I}$  using Iodogen, with an immunoreactive fraction of 76%.  $^{125}\text{I}$ -NZ-1(Iodogen) exhibited  $K_D$  values of  $2.58 \times 10^{-9}$  and  $9.79 \times 10^{-10}$  (mol/L) against LN319 and D397MG, respectively, indicating that NZ-1 also has high affinity against podoplanin-expressing glioblastoma cells.

#### 3.3. Internalization of $^{125}\text{I}$ -NZ-1(Iodogen) by D397MG and LN319 glioblastoma cells

An internalization assay was performed in a single-label format using  $^{125}\text{I}$ -NZ-1(Iodogen) and the podoplanin-positive glioblastoma cells, D397MG and LN319. The immunoreactive fraction of  $^{125}\text{I}$ -NZ-1(Iodogen) was 76%. Cell surface-bound counts and culture supernatant counts in D397MG showed little change over time (Fig. 2A), whereas

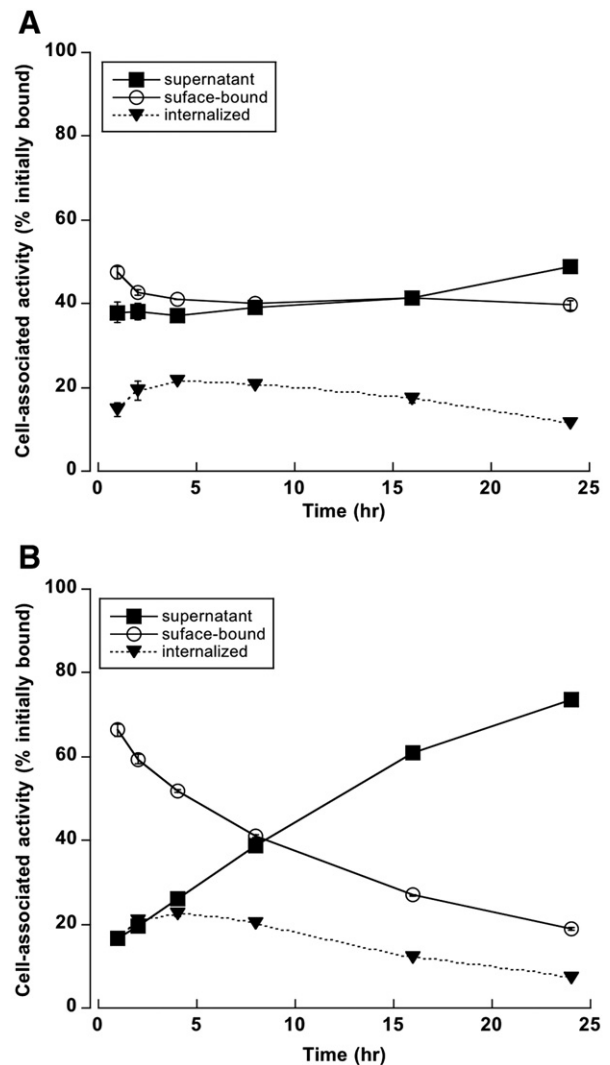


Fig. 2. Internalization of NZ-1 into glioblastoma cells. D397MG (A) and LN319 (B) cells were incubated with  $^{125}\text{I}$ -NZ-1(Iodogen) at 4°C for 1 h and then washed with fresh medium to remove unbound radioactivity. Cells were cultured at 0, 1, 2, 4, 8, 16 and 24 h at 37°C and processed at various time periods.

cell surface-bound counts in LN319 gradually decreased, accompanied by a slow increase in counts in the cell culture supernatant (Fig. 2B). The intracellularly trapped radioactivity of  $^{125}\text{I}$ -NZ-1(Iodogen) in D397MG cells gradually increased to a maximum of  $21.6 \pm 0.3\%$  at the 4-h time point (Fig. 2A). A similar trend was seen in LN319 cells with  $22.4 \pm 0.5\%$  of initially bound radioactivity within the cells at 4 h (Fig. 2B).

3.4. Paired-label internalization of NZ-1 by LN319 cells: Iodogen vs. SGMIB

The internalization of  $^{125}\text{I}$ -NZ-1(Iodogen) and [ $^{131}\text{I}$ ]SGMIB-NZ-1 by LN319 cells was compared in paired-label format after binding during 1-h incubation at 4°C. The immunoreactive fraction was 62% and 55% for  $^{125}\text{I}$ -

NZ-1(Iodogen) and [ $^{131}\text{I}$ ]SGMIB-NZ-1, respectively. At every time point studied, the percentage of the radioiodine activity initially bound to the cells for [ $^{131}\text{I}$ ]SGMIB-NZ-1 (Fig. 3B) that was present in the intracellular compartment was significantly higher ( $P < .01$ ) than that for  $^{125}\text{I}$ -NZ-1 (Iodogen) (Fig. 3A). The percent of radioactivity retained intracellularly for  $^{125}\text{I}$ -NZ-1(Iodogen) peaked at 1 h ( $13.8 \pm 0.6\%$ ) and declined thereafter (Fig. 3A). In contrast, internalized radioactivity peaked at 8 h ( $26.3 \pm 0.8\%$ ) with [ $^{131}\text{I}$ ]SGMIB-NZ-1 (Fig. 3B). At this time point, the intracellularly trapped  $^{131}\text{I}$  activity was more than 2.5 times higher than the  $^{125}\text{I}$  activity ( $9.95 \pm 0.15\%$ ). To confirm this result, internalization assay using the D2159MG xenograft cells was also performed. The immunoreactive fraction of [ $^{125}\text{I}$ ]SGMIB-NZ-1 was 75%. As shown in Fig. 4, cell surface-bound counts for D2159MG gradually decreased, accompanied by a slow increase in counts in the cell culture supernatant. The internalization of [ $^{125}\text{I}$ ]SGMIB-NZ-1 into D2159MG cells gradually increased to a maximum of  $30.7 \pm 2.0\%$  at 16 h, suggesting that [ $^{125}\text{I}$ ]SGMIB-NZ-1 was also internalized effectively into D2159MG xenograft cells.

3.5. Biodistribution of NZ-1 in D2159MG xenograft: Iodogen vs. SGMIB

A paired-label biodistribution experiment was performed in athymic mice bearing D2159MG human glioblastoma xenograft to directly compare the tumor and normal organ distribution of an anti-podoplanin mAb NZ-1 radioiodinated using Iodogen and SGMIB methods. The immunoreactive fraction was 62% and 55%, respectively. No growth of these D2159MG xenografts was seen during the course of the experiments. The mean tumor weight harvested at necropsy on the first day was  $0.46 \pm 0.20$  g, whereas that on the

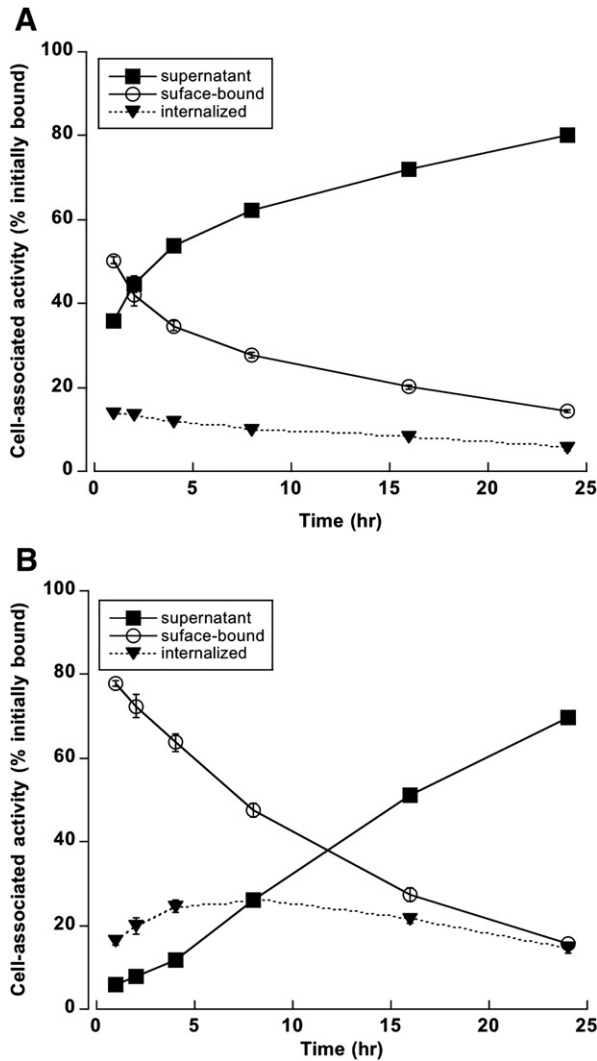


Fig. 3. Paired-label internalization of  $^{125}\text{I}$ -NZ-1(Iodogen) and [ $^{131}\text{I}$ ]SGMIB-NZ-1 in LN319 cells. LN319 cells were incubated with  $^{125}\text{I}$ -NZ-1(Iodogen) (A) or [ $^{131}\text{I}$ ]SGMIB-NZ-1 (B) at 4°C for 1 h and then washed with fresh medium to remove unbound radioactivity. Cells were cultured at 0, 1, 2, 4, 8, 16 and 24 h at 37°C and processed at various time periods.

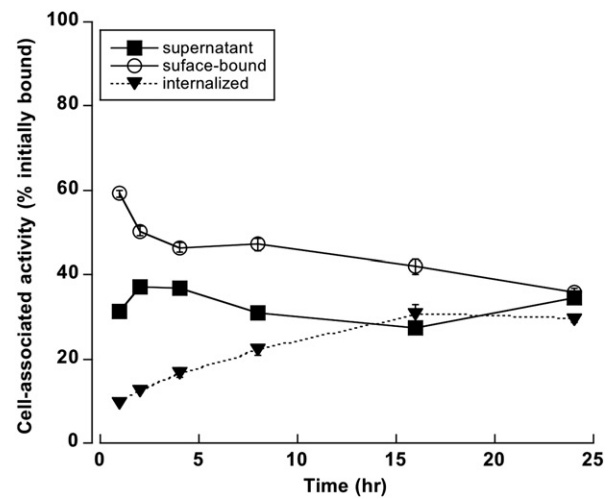


Fig. 4. Internalization of [ $^{125}\text{I}$ ]SGMIB-NZ-1 in D2159MG xenograft cells. D2159MG cells were incubated with [ $^{125}\text{I}$ ]SGMIB-NZ-1 at 4°C for 1 h and washed with fresh medium to remove unbound radioactivity. Cells were cultured at 0, 1, 2, 4, 8, 16 and 24 h at 37°C and processed at various time periods.

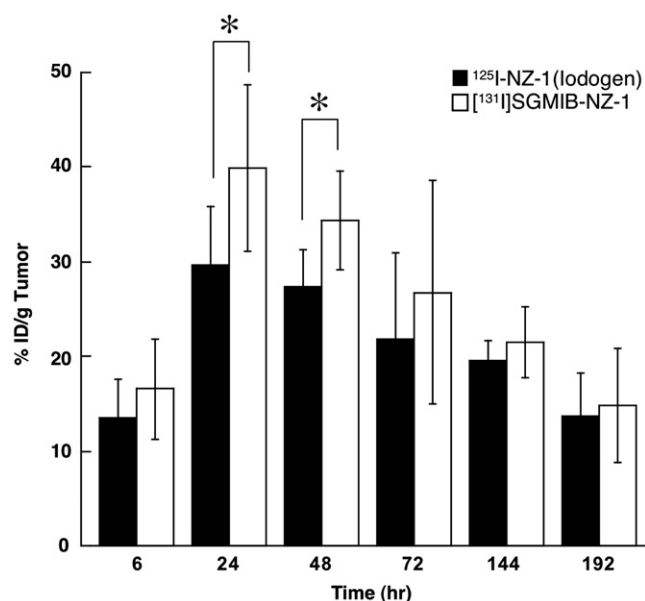


Fig. 5. Paired-label uptake of  $^{125}\text{I}$ -NZ-1 (Iodogen) or  $^{131}\text{I}$ ]SGMIB-NZ-1 in athymic mice hosting D2159MG xenografts. Values given are %ID/g (mean  $\pm$  S.D.). An asterisk indicates that differences were statistically significant ( $P < .05$ ) by an unpaired Student's  $t$  test.

eighth day was  $0.45 \pm 0.19$  g. As shown in Fig. 5, the tumor accumulation of radioiodine activity (%ID/g) of  $^{131}\text{I}$ ]SGMIB-NZ-1 was significantly higher than that of  $^{125}\text{I}$ -NZ-1 (Iodogen) ( $P < .05$ ) at 24 h ( $39.9 \pm 8.8$  %ID/g vs.  $29.7 \pm 6.1$  %ID/g) and 48 h ( $34.4 \pm 5.2$  %ID/g vs.  $27.4 \pm 4.0$  %ID/g). Data for uptake in normal tissues are given in Table 1. Except at early time points for a few tissues, the uptake of radioactivity from  $^{131}\text{I}$ ]SGMIB-NZ-1 was generally lower. Liver and spleen demonstrated slightly higher uptake at 6 h. The thyroid uptake of radioactivity from  $^{131}\text{I}$ ]SGMIB-NZ-1 was substantially lower than that from  $^{125}\text{I}$ -NZ-1 (Iodogen) at all time points. Higher uptake in tumor and concomitant lower uptake in normal tissues resulted in higher tumor-to-tissue ratios for  $^{131}\text{I}$ ]SGMIB-NZ-1 (data for selected tissues given in Fig. 6).

To determine the specificity of uptake in D2159MG tumor in vivo, the biodistribution assay of NZ-1 labeled with SGMIB ( $^{125}\text{I}$ ]SGMIB-NZ-1) was repeated. The immunoreactive fraction of  $^{125}\text{I}$ ]SGMIB-NZ-1 was 75%. No growth of these D2159MG xenografts was seen during the course of the experiments. The mean tumor weight harvested at necropsy on the first day was  $0.98 \pm 0.19$  g, whereas it was  $0.68 \pm 0.29$  g on the second day. As shown in Fig. 7, the tumor accumulation of radioiodine activity from  $^{125}\text{I}$ ]SGMIB-NZ-1 was significantly reduced at all time points

Table 1  
Biodistribution of  $^{125}\text{I}$ -NZ-1 (Iodogen) and  $^{131}\text{I}$ ]SGMIB-NZ-1 in athymic mice bearing D2159MG xenografts<sup>a</sup>

Tissue	6 h	24 h	48 h	72 h	144 h	192 h
<i><math>^{125}\text{I}</math>-NZ-1 (Iodogen)</i>						
Liver	6.85 $\pm$ 0.76	3.91 $\pm$ 1.06	2.46 $\pm$ 0.77	1.34 $\pm$ 0.47	1.08 $\pm$ 0.27	0.93 $\pm$ 0.28
Spleen	4.20 $\pm$ 0.68	2.47 $\pm$ 0.58	1.76 $\pm$ 0.27	1.14 $\pm$ 0.61	0.97 $\pm$ 0.12	0.61 $\pm$ 0.18
Lungs	8.90 $\pm$ 0.93	7.77 $\pm$ 2.14	4.46 $\pm$ 0.88	2.98 $\pm$ 1.45	2.07 $\pm$ 0.82	1.63 $\pm$ 0.56
Heart	6.01 $\pm$ 0.95	4.89 $\pm$ 0.99	3.36 $\pm$ 0.38	1.88 $\pm$ 0.96	1.71 $\pm$ 0.23	1.18 $\pm$ 0.20
Kidneys	6.71 $\pm$ 0.88	4.39 $\pm$ 1.71	2.25 $\pm$ 0.64	1.69 $\pm$ 0.79	1.35 $\pm$ 0.34	0.71 $\pm$ 0.18
Stomach	4.11 $\pm$ 1.23	1.63 $\pm$ 0.56	0.95 $\pm$ 0.30	0.56 $\pm$ 0.25	0.64 $\pm$ 0.08	0.26 $\pm$ 0.08
Small intestine	2.35 $\pm$ 0.34	1.54 $\pm$ 0.35	0.85 $\pm$ 0.10	0.51 $\pm$ 0.26	0.49 $\pm$ 0.05	0.28 $\pm$ 0.09
Large intestine	1.27 $\pm$ 0.18	0.96 $\pm$ 0.19	0.53 $\pm$ 0.04	0.33 $\pm$ 0.14	0.29 $\pm$ 0.05	0.18 $\pm$ 0.05
Thyroid	0.63 $\pm$ 0.13	0.46 $\pm$ 0.47	1.01 $\pm$ 0.29	1.20 $\pm$ 0.19	1.86 $\pm$ 0.45	1.36 $\pm$ 0.14
Muscle	0.89 $\pm$ 0.26	1.38 $\pm$ 0.20	0.93 $\pm$ 0.05	0.52 $\pm$ 0.19	0.47 $\pm$ 0.07	0.29 $\pm$ 0.10
Blood	20.62 $\pm$ 1.55	14.95 $\pm$ 3.48	10.14 $\pm$ 1.79	6.32 $\pm$ 2.41	5.55 $\pm$ 0.80	3.76 $\pm$ 0.89
Bone	1.57 $\pm$ 0.51	1.49 $\pm$ 0.37	1.17 $\pm$ 0.42	0.72 $\pm$ 0.27	0.58 $\pm$ 0.03	0.35 $\pm$ 0.09
Brain	0.38 $\pm$ 0.13	0.26 $\pm$ 0.09	0.25 $\pm$ 0.07	0.23 $\pm$ 0.13	0.16 $\pm$ 0.02	0.12 $\pm$ 0.03
<i><math>^{131}\text{I}</math>]SGMIB-NZ-1</i>						
Liver	8.38 $\pm$ 1.32	3.98 $\pm$ 1.21	2.39 $\pm$ 1.06	1.02 $\pm$ 0.42	0.83 $\pm$ 0.20	0.60 $\pm$ 0.18
Spleen	4.78 $\pm$ 1.04	2.55 $\pm$ 0.59	1.83 $\pm$ 0.24	1.01 $\pm$ 0.54	0.77 $\pm$ 0.16	0.48 $\pm$ 0.09
Lungs	7.48 $\pm$ 0.59	6.46 $\pm$ 1.81	3.13 $\pm$ 0.79	1.90 $\pm$ 1.13	1.17 $\pm$ 0.51	0.88 $\pm$ 0.37
Heart	5.62 $\pm$ 0.86	4.10 $\pm$ 0.94	2.52 $\pm$ 0.36	1.20 $\pm$ 0.79	1.02 $\pm$ 0.19	0.63 $\pm$ 0.12
Kidneys	6.54 $\pm$ 1.01	3.95 $\pm$ 1.56	1.78 $\pm$ 0.58	1.12 $\pm$ 0.71	0.84 $\pm$ 0.26	0.38 $\pm$ 0.12
Stomach	1.25 $\pm$ 0.16	0.72 $\pm$ 0.30	0.25 $\pm$ 0.09	0.12 $\pm$ 0.08	0.24 $\pm$ 0.07	0.08 $\pm$ 0.03
Small intestine	2.63 $\pm$ 0.36	1.49 $\pm$ 0.41	0.74 $\pm$ 0.14	0.38 $\pm$ 0.24	0.36 $\pm$ 0.02	0.18 $\pm$ 0.05
Large intestine	1.87 $\pm$ 0.24	1.07 $\pm$ 0.20	0.57 $\pm$ 0.08	0.32 $\pm$ 0.13	0.28 $\pm$ 0.04	0.19 $\pm$ 0.09
Thyroid	0.45 $\pm$ 0.15	0.14 $\pm$ 0.17	0.15 $\pm$ 0.05	0.11 $\pm$ 0.05	0.11 $\pm$ 0.04	0.08 $\pm$ 0.05
Muscle	0.72 $\pm$ 0.21	1.15 $\pm$ 0.20	0.72 $\pm$ 0.08	0.34 $\pm$ 0.17	0.29 $\pm$ 0.04	0.17 $\pm$ 0.08
Blood	17.54 $\pm$ 1.49	11.25 $\pm$ 3.26	6.84 $\pm$ 1.67	3.36 $\pm$ 1.83	3.04 $\pm$ 0.48	1.86 $\pm$ 0.52
Bone	1.50 $\pm$ 0.46	1.33 $\pm$ 0.25	1.04 $\pm$ 0.40	0.53 $\pm$ 0.24	0.38 $\pm$ 0.03	0.24 $\pm$ 0.06
Brain	0.31 $\pm$ 0.11	0.21 $\pm$ 0.06	0.17 $\pm$ 0.06	0.14 $\pm$ 0.10	0.10 $\pm$ 0.01	0.07 $\pm$ 0.02

<sup>a</sup> Values are mean %ID/g $\pm$ S.D. ( $n=5$  for 6, 24 and 48 h;  $n=4$  for 72, 144 and 192 h) except for thyroid for which %ID/organ is used.

Table 2  
Biodistribution of [<sup>125</sup>I]SGMIB-NZ-1 and [<sup>125</sup>I]SGMIB-NZ-1+-NZ-1 in athymic mice bearing D2159MG xenografts<sup>a</sup>

Tissue	Percent injected dose per gram					
	6 h		24 h		48 h	
	[ <sup>125</sup> I]SGMIB-NZ-1	[ <sup>125</sup> I]SGMIB-NZ-1 + cold NZ-1	[ <sup>125</sup> I]SGMIB-NZ-1	[ <sup>125</sup> I]SGMIB-NZ-1 + cold NZ-1	[ <sup>125</sup> I]SGMIB-NZ-1	[ <sup>125</sup> I]SGMIB-NZ-1 + cold NZ-1
Liver	5.92±2.40	5.75±1.27	2.68±0.74	2.89±0.52	1.68±0.57	2.42±0.40
Spleen	4.75±2.34	3.97±0.66	2.00±0.46	2.44±0.48	1.38±0.58	1.77±0.23
Lungs	11.35±5.16	11.27±2.98	5.23±0.97	6.73±0.99	3.67±1.44	5.21±0.91
Heart	4.05±1.22	5.23±0.81	2.56±0.54	3.66±1.06	1.78±0.78	2.47±0.27
Kidneys	4.40±0.70	5.56±0.66	2.61±0.77	3.46±0.71	1.78±0.70	2.76±0.28
Stomach	0.94±0.40	1.20±0.39	0.41±0.19	0.44±0.16	0.28±0.13	0.54±0.12
Small intestine	1.52±0.13	2.31±0.43	0.83±0.21	1.03±0.15	0.64±0.26	0.97±0.09
Large intestine	1.31±0.15	1.62±0.43	0.63±0.17	0.68±0.14	0.45±0.16	0.69±0.18
Thyroid	0.40±0.19	0.54±0.18	0.20±0.11	0.24±0.10	0.17±0.05	0.24±0.06
Muscle	1.03±0.27	1.05±0.15	0.96±0.18	1.28±0.16	0.67±0.21	0.93±0.10
Blood	15.20±2.39	19.03±2.54	8.35±2.20	12.08±2.29	5.68±2.18	9.13±0.71
Bone	1.41±0.21	1.72±0.40	1.12±0.44	1.33±0.23	0.82±0.21	1.08±0.20
Brain	0.48±0.07	0.60±0.08	0.31±0.10	0.42±0.10	0.23±0.04	0.33±0.12

<sup>a</sup> Values are mean %ID/g±S.D. (*n*=5) except for thyroid for which %ID/organ is used.

when mice were co-injected with 100-fold excess of unlabeled NZ-1 (*P*<.01). Data for uptake in normal tissues are given in Table 2.

#### 4. Discussion

The purpose of this study was to determine the affinity of anti-podoplanin antibody NZ-1 and to investigate whether NZ-1 is suitable for therapy against malignant gliomas by performing internalization assays in vitro using glioblastoma cells as well as biodistribution experiments in vivo using glioblastoma xenograft models. To determine the affinity of NZ-1, we performed a kinetic analysis of the interaction of NZ-1 with podoplanin peptide by surface plasmon resonance and we also performed Scatchard analysis using podoplanin-positive glioblastoma cells. *K<sub>D</sub>* was determined to be about 0.1 nM in BIAcore and about 1 nM in Scatchard analysis, indicating that NZ-1 has high affinity against both podoplanin peptide and glioblastoma cells. This high affinity of NZ-1 should be sufficient for antibody-based immunotherapy, because the affinity of NZ-1 was much higher than that of anti-epidermal growth factor receptor-vIII (EGFRvIII) scFv MR1-1 [38] and was similar to that of mouse anti-EGFRvIII mAb L8A4 [39]. The binding site barrier is an important theoretical concept in antibody targeting because it suggests that if the on-rate for binding to the tumor molecular target is too high, it will impede delivery of the antibody to regions of the tumor that are distant from vascular supply [40]. Although the affinity of NZ-1 binding to podoplanin peptide was 0.12 nM, the *K<sub>D</sub>* determined by cell-based Scatchard analysis was an order of magnitude higher, 1.0–2.6 nM. It is difficult to determine whether a dissociation constant in this range will result in inhomogeneous delivery to tumor due to binding site barrier-related effects. However, the impact of this potential issue should be

minimized in the clinical settings of minimum residual disease where we anticipate applying radiolabeled NZ-1–post-surgical glioblastoma and neoplastic meningitis.

Initially, NZ-1 was radioiodinated by the direct electrophilic method using Iodogen as the oxidant. It is not known whether the NZ-1–podoplanin complex will undergo internalization once NZ-1 binds to podoplanin. To investigate this and to have a stably radioiodinated NZ-1, it was also radioiodinated using SGMIB, one of the residualizing agents that we have developed for radiolabeling mAbs that undergo extensive internalization [34]. Indeed, it was possible to radioiodinate NZ-1 in reasonable yields with the preservation of immunoreactivity.

Multiple models were utilized to confirm that the behavior of NZ-1 was not unique to a particular cell line. Internalization experiments were performed using two podoplanin-positive glioblastoma cell lines, D397MG and LN319, as well as cells obtained by dissociation of one podoplanin-positive glioblastoma xenograft, D2159MG. These three glioblastoma cells have different characters both in vitro and in vivo. For example, LN319 cells grow two to three times faster than both D397MG and D2159MG cells in vitro. LN319 has no tumorigenicity, whereas D397MG and D2159MG cells grow very well in vivo. However, the podoplanin expression of D397MG cells was extremely decreased in vivo, making it impractical to perform in vivo targeting experiments with this cell line. As shown in Fig. 2, <sup>125</sup>I-NZ-1(Iodogen) was internalized into D397MG and LN319 cells. Interestingly, cell surface-bound counts in LN319 gradually decreased, accompanied by a slow increase in counts in the cell culture supernatant (Figs. 2B and 3), whereas D397MG showed little change over time (Fig. 2A), which might reflect differences in growth rate, metabolism, shedding or recycling. We further compared the internalization of <sup>125</sup>I-NZ-1(Iodogen) with that of [<sup>131</sup>I]SGMIB-NZ-1 using LN319, because we have previously demonstrated the

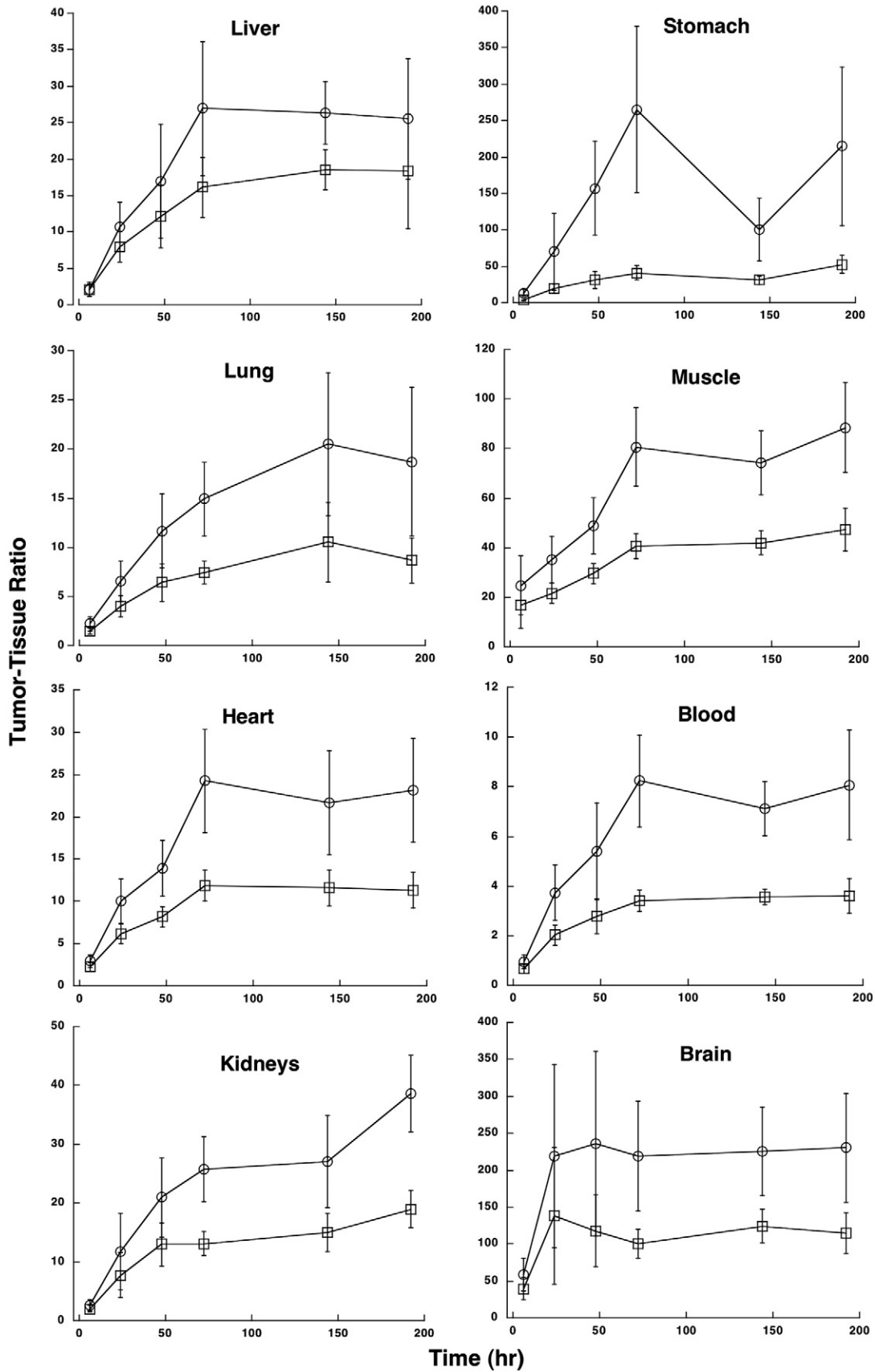


Fig. 6. Tumor-to-tissue ratios observed in athymic mice bearing D2159MG xenografts and injected with  $^{125}\text{I}$ -NZ-1 (Iodogen) (square) and  $[^{131}\text{I}]$ SGMIB-NZ-1 (circle).

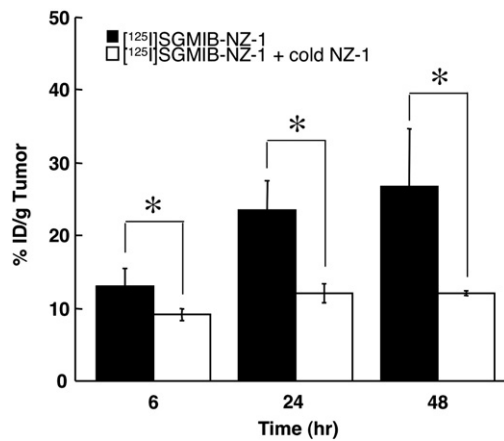


Fig. 7. Biodistribution of [ $^{125}\text{I}$ ]SGMIB-NZ-1 in D2159MG. Uptake of [ $^{125}\text{I}$ ]SGMIB-NZ-1 and [ $^{125}\text{I}$ ]SGMIB-NZ-1+100-fold nonlabeled NZ-1 in athymic mice hosting D2159MG xenografts. Values given are %ID/g (mean  $\pm$  S.D.). An asterisk indicates that differences were statistically significant ( $P < 0.01$ ) by unpaired Student's  $t$  test.

advantages of labeling with SGMIB for the efficient delivery of halogen radionuclides attached to mAbs that undergo internalization in tumor cells [34]. For example, paired-label in vitro internalization assays using EGFRvIII-expressing U87MG cells demonstrated that the amount of radioactivity retained in cells after internalization for EGFRvIII-specific L8A4 labeled with [ $^{131}\text{I}$ ]SGMIB was three to four times higher than that for L8A4 labeled with  $^{125}\text{I}$  using Iodogen. Likewise, the internalization of radioiodine activity of [ $^{131}\text{I}$ ]SGMIB-NZ-1 ( $26.3 \pm 0.8\%$  at 8 h) was significantly higher than that of  $^{125}\text{I}$ -NZ-1 (Iodogen) ( $10.0 \pm 0.2\%$  at 8 h) in LN319 cells with more than 2.5 times higher intracellular activity observed with SGMIB labeling at later time points (Fig. 3A and B). The internalization of [ $^{125}\text{I}$ ]SGMIB-NZ-1 into D2159MG xenograft cells was also considerably higher, with  $30.7 \pm 2.0\%$  of initially bound radioactivity in the intracellular compartments at the 16-h time point (Fig. 4). These results are similar to results seen with the anti-EGFRvIII mAb L8A4 radioiodinated with this prosthetic group and other cell lines [41], suggesting that NZ-1 does indeed become internalized once it binds to podoplanin.

Next, we performed biodistribution of NZ-1 in athymic mice bearing the D2159MG glioblastoma xenograft. We could not obtain LN319 xenograft in athymic mice because of its low tumorigenicity, and the podoplanin expression was extremely decreased in D397MG xenograft. Both  $^{125}\text{I}$ -NZ-1 (Iodogen) and [ $^{131}\text{I}$ ]SGMIB-NZ-1 were well accumulated into tumors, and the tumor accumulation of radioiodine activity of [ $^{131}\text{I}$ ]SGMIB-NZ-1 was significantly higher ( $P < 0.05$ ) than that of  $^{125}\text{I}$ -NZ-1 (Iodogen) at time points of 24 and 48 h (Fig. 5), which is consistent with the data obtained from internalization assay in vitro. The absolute tumor uptake of [ $^{131}\text{I}$ ]SGMIB-NZ-1 is similar to that seen earlier for mAb L8A4 labeled using SGMIB in a different xenograft model [42]. Furthermore, reduction in tumor uptake when a large excess of unlabeled NZ-1 was present

indicates that the uptake is indeed due to the specific binding of NZ-1 to podoplanin (Fig. 7). As seen in the past for mAbs radioiodinated with acylation agents in general, and SGMIB in particular, the thyroid uptake of radioactivity from [ $^{131}\text{I}$ ]SGMIB-NZ-1 was substantially lower than that from  $^{125}\text{I}$ -NZ-1 (Iodogen), which again demonstrates inertness of this prosthetic group for in vivo dehalogenation. Lower uptake in blood and other normal tissues, along with the resultant higher tumor-to-normal tissue ratios for [ $^{131}\text{I}$ ]SGMIB-NZ-1, makes this mAb a potential tool in the targeted immunotherapy of gliomas (Fig. 6). Collectively, these results suggest that NZ-1 should be suitable for targeted radioimmunotherapy of glioblastomas.

In conclusion, the rat anti-podoplanin mAb NZ-1 showed high affinity against not only podoplanin peptide but also glioblastoma cells. Furthermore,  $^{125}\text{I}$ -NZ-1 (Iodogen) was internalized into glioblastoma cells in vitro. Paired-label internalization assays indicated that [ $^{131}\text{I}$ ]SGMIB-NZ-1 showed higher retention of radioactivity compared to  $^{125}\text{I}$ -NZ-1 (Iodogen). Likewise, tumor uptake of radioactivity in athymic mice bearing D2159MG xenografts in vivo was significantly higher for [ $^{131}\text{I}$ ]SGMIB-NZ-1 than for  $^{125}\text{I}$ -NZ-1 (Iodogen). Taken together, these results demonstrate the potential utility of an anti-podoplanin antibody NZ-1 in antibody-based therapy against glioblastoma.

## Acknowledgments

We thank Donna Affleck, Philip Welsh, Xiao-Guang Zhao and Scott E. Szafranski of Duke University Medical Center for their excellent technical assistance. We also thank Chifumi Kitanaka of Yamagata University School of Medicine for his helpful suggestions.

## References

- [1] DeAngelis LM. Brain tumors. *N Engl J Med* 2001;344:114–23.
- [2] Wong AJ, Bigner SH, Bigner DD, Kinzler KW, Hamilton SR, Vogelstein B. Increased expression of the epidermal growth factor receptor gene in malignant gliomas is invariably associated with gene amplification. *Proc Natl Acad Sci U S A* 1987;84:6899–903.
- [3] Wikstrand CJ, Hale LP, Batra SK, Hill ML, Humphrey PA, Kurpad SN, et al. Monoclonal antibodies against EGFRvIII are tumor specific and react with breast and lung carcinomas and malignant gliomas. *Cancer Res* 1995;55:3140–8.
- [4] Wikstrand CJ, He XM, Fuller GN, Bigner SH, Fredman P, Svennerholm L, et al. Occurrence of lacto series gangliosides 3'-isoLM1 and 3',6'-isoLD1 in human gliomas in vitro and in vivo. *J Neuropathol Exp Neurol* 1991;50:756–69.
- [5] Zalutsky MR, Moseley RP, Coakham HB, Coleman RE, Bigner DD. Pharmacokinetics and tumor localization of  $^{131}\text{I}$ -labeled anti-tenascin monoclonal antibody 81C6 in patients with gliomas and other intracranial malignancies. *Cancer Res* 1989;49:2807–13.
- [6] Zalutsky MR, Moseley RP, Benjamin JC, Colapinto EV, Fuller GN, Coakham HP, et al. Monoclonal antibody and F(ab')<sub>2</sub> fragment delivery to tumor in patients with glioma: comparison of intracarotid and intravenous administration. *Cancer Res* 1990;50:4105–10.
- [7] Kato Y, Kuan CT, Chang J, Kaneko MK, Ayriss J, Piao H, et al. GMab-1, a high-affinity anti-3'-isoLM1/3',6'-isoLD1 IgG monoclonal

- antibody, raised in lacto-series ganglioside-defective knockout mice. *Biochem Biophys Res Commun* 2010;391:750–5.
- [8] Kato Y, Fujita N, Kunita A, Sato S, Kaneko M, Osawa M, et al. Molecular identification of aggrus/T1alpha as a platelet aggregation-inducing factor expressed in colorectal tumors. *J Biol Chem* 2003;278:51599–605.
- [9] Kaneko MK, Kato Y, Kitano T, Osawa M. Conservation of a platelet activating domain of aggrus/podoplanin as a platelet aggregation-inducing factor. *Gene* 2006;378:52–7.
- [10] Kaneko M, Kato Y, Kunita A, Fujita N, Tsuruo T, Osawa M. Functional sialylated *O*-glycan to platelet aggregation on aggrus (T1alpha/podoplanin) molecules expressed in Chinese hamster ovary cells. *J Biol Chem* 2004;279:38838–43.
- [11] Kaneko MK, Kato Y, Kameyama A, Ito H, Kuno A, Hirabayashi J, et al. Functional glycosylation of human podoplanin: glycan structure of platelet aggregation-inducing factor. *FEBS Lett* 2007;581:331–6.
- [12] Kato Y, Kaneko M, Sata M, Fujita N, Tsuruo T, Osawa M. Enhanced expression of aggrus (T1alpha/podoplanin), a platelet-aggregation-inducing factor in lung squamous cell carcinoma. *Tumor Biol* 2005;26:195–200.
- [13] Martin-Villar E, Scholl FG, Gamallo C, Yurrita MM, Munoz-Guerra M, Cruces J, et al. Characterization of human PA2.26 antigen (T1alpha-2, podoplanin), a small membrane mucin induced in oral squamous cell carcinomas. *Int J Cancer* 2005;113:899–910.
- [14] Dumoff KL, Chu CS, Harris EE, Holtz D, Xu X, Zhang PJ, et al. Low podoplanin expression in pretreatment biopsy material predicts poor prognosis in advanced-stage squamous cell carcinoma of the uterine cervix treated by primary radiation. *Mod Pathol* 2006;19:708–16.
- [15] Wicki A, Lehembre F, Wick N, Hantusch B, Kerjaschki D, Christofori G. Tumor invasion in the absence of epithelial–mesenchymal transition: podoplanin-mediated remodeling of the actin cytoskeleton. *Cancer Cell* 2006;9:261–72.
- [16] Vormittag L, Thumher D, Geleff S, Pammer J, Heiduschka G, Brunner M, et al. Co-expression of Bmi-1 and podoplanin predicts overall survival in patients with squamous cell carcinoma of the head and neck treated with radio(chemo)therapy. *Int J Radiat Oncol Biol Phys* 2009;73:913–8.
- [17] Ito T, Ishii G, Nagai K, Nagano T, Kojika M, Murata Y, et al. Low podoplanin expression of tumor cells predicts poor prognosis in pathological stage IB squamous cell carcinoma of the lung, tissue microarray analysis of 136 patients using 24 antibodies. *Lung Cancer* 2009;63:418–24.
- [18] Rahadiani N, Ikeda JI, Makino T, Tian T, Qiu Y, Mamat S, Wang Y, Doki Y, Aozasa K, Morii E. Tumorigenic role of podoplanin in esophageal squamous-cell carcinoma. *Ann Surg Oncol* 2010;17:1311–23.
- [19] Kato Y, Sasagawa I, Kaneko M, Osawa M, Fujita N, Tsuruo T. Aggrus: a diagnostic marker that distinguishes seminoma from embryonal carcinoma in testicular germ cell tumors. *Oncogene* 2004;23:8552–6.
- [20] Suzuki H, Kato Y, Kaneko MK, Okita Y, Narimatsu H, Kato M. Induction of podoplanin by transforming growth factor-beta in human fibrosarcoma. *FEBS Lett* 2008;582:341–5.
- [21] Mishima K, Kato Y, Kaneko MK, Nakazawa Y, Kunita A, Fujita N, et al. Podoplanin expression in primary central nervous system germ cell tumors: a useful histological marker for the diagnosis of germinoma. *Acta Neuropathol (Berl)* 2006;111:563–8.
- [22] Mishima K, Kato Y, Kaneko MK, Nishikawa R, Hirose T, Matsutani M. Increased expression of podoplanin in malignant astrocytic tumors as a novel molecular marker of malignant progression. *Acta Neuropathol (Berl)* 2006;111:483–8.
- [23] Kato Y, Kaneko MK, Kuno A, Uchiyama N, Amano K, Chiba Y, et al. Inhibition of tumor cell-induced platelet aggregation using a novel anti-podoplanin antibody reacting with its platelet-aggregation-stimulating domain. *Biochem Biophys Res Commun* 2006;349:1301–7.
- [24] Kunita A, Kashima TG, Morishita Y, Fukayama M, Kato Y, Tsuruo T, et al. The platelet aggregation-inducing factor aggrus/podoplanin promotes pulmonary metastasis. *Am J Pathol* 2007;170:1337–47.
- [25] Kato Y, Kaneko MK, Kunita A, Ito H, Kameyama A, Ogasawara S, et al. Molecular analysis of the pathophysiological binding of the platelet aggregation-inducing factor podoplanin to the C-type lectin-like receptor CLEC-2. *Cancer Sci* 2008;99:54–61.
- [26] Martin-Villar E, Megias D, Castel S, Yurrita MM, Vilaro S, Quintanilla M. Podoplanin binds ERM proteins to activate RhoA and promote epithelial–mesenchymal transition. *J Cell Sci* 2006;119:4541–53.
- [27] Kawase A, Ishii G, Nagai K, Ito T, Nagano T, Murata Y, et al. Podoplanin expression by cancer associated fibroblasts predicts poor prognosis of lung adenocarcinoma. *Int J Cancer* 2008;123:1053–9.
- [28] Kawaguchi H, El-Naggar AK, Papadimitrakopoulou V, Ren H, Fan YH, Feng L, et al. Podoplanin: a novel marker for oral cancer risk in patients with oral premalignancy. *J Clin Oncol* 2008;26:354–60.
- [29] Singh SK, Hawkins C, Clarke ID, Squire JA, Bayani J, Hide T, et al. Identification of human brain tumour initiating cells. *Nature* 2004;432:396–401.
- [30] Bao S, Wu Q, McLendon RE, Hao Y, Shi Q, Hjelmeland AB, et al. Glioma stem cells promote radioresistance by preferential activation of the DNA damage response. *Nature* 2006;444:756–60.
- [31] Hambardzumyan D, Squatrito M, Holland EC. Radiation resistance and stem-like cells in brain tumors. *Cancer Cell* 2006;10:454–6.
- [32] Atsumi N, Ishii G, Kojima M, Sanada C, Fujii S, Ochiai A. Podoplanin, a novel marker of tumor-initiating cells in human squamous cell carcinoma A431. *Biochem Biophys Res Commun* 2008;373:36–41.
- [33] Ogasawara S, Kaneko MK, Price JE, Kato Y. Characterization of anti-podoplanin monoclonal antibodies: critical epitopes for neutralizing the interaction between podoplanin and CLEC-2. *Hybridoma* 2008;27:259–67.
- [34] Vaidyanathan G, Affleck DJ, Li J, Welsh P, Zalutsky MRA. Polar substituent-containing acylation agent for the radioiodination of internalizing monoclonal antibodies: *N*-succinimidyl 4-guanidinomethyl-3-<sup>131</sup>Iiodobenzoate ([<sup>131</sup>I]SGMIB). *Bioconjug Chem* 2001;12:428–38.
- [35] Zalutsky MR, Zhao XG, Alston KL, Bigner D. High-level production of alpha-particle-emitting (211)At and preparation of (211)At-labeled antibodies for clinical use. *J Nucl Med* 2001;42:1508–15.
- [36] Lindmo T, Boven E, Cuttitta F, Fedorko J, Bunn Jr PA. Determination of the immunoreactive fraction of radiolabeled monoclonal antibodies by linear extrapolation to binding at infinite antigen excess. *J Immunol Methods* 1984;72:77–89.
- [37] Friedman HS, Colvin OM, Skapek SX, Ludeman SM, Elion GB, Schold Jr SC, et al. Experimental chemotherapy of human medulloblastoma cell lines and transplantable xenografts with bifunctional alkylating agents. *Cancer Res* 1988;48:4189–95.
- [38] Beers R, Chowdhury P, Bigner D, Pastan I. Immunotoxins with increased activity against epidermal growth factor receptor vIII-expressing cells produced by antibody phage display. *Clin Cancer Res* 2000;6:2835–43.
- [39] Reist CJ, Archer GE, Kurpad SN, Wikstrand CJ, Vaidyanathan G, Willingham MC, et al. Tumor-specific anti-epidermal growth factor receptor variant III monoclonal antibodies: use of the tyramine-cellobiose radioiodination method enhances cellular retention and uptake in tumor xenografts. *Cancer Res* 1995;55:4375–82.
- [40] Saga T, Neumann RD, Heya T, Sato J, Kinuya S, Le N, et al. Targeting cancer micrometastases with monoclonal antibodies: a binding-site barrier. *Proc Natl Acad Sci U S A* 1995;92:8999–9003.
- [41] Vaidyanathan G, Affleck DJ, Bigner DD, Zalutsky MR. *N*-Succinimidyl 3-[<sup>211</sup>At]astato-4-guanidinomethylbenzoate: an acylation agent for labeling internalizing antibodies with alpha-particle emitting <sup>211</sup>At. *Nucl Med Biol* 2003;30:351–9.
- [42] Vaidyanathan G, Affleck DJ, Bigner DD, Zalutsky MR. Improved xenograft targeting of tumor-specific anti-epidermal growth factor receptor variant III antibody labeled using *N*-succinimidyl 4-guanidinomethyl-3-iodobenzoate. *Nucl Med Biol* 2002;29:1–11.